

# Evaluating Temperature Scaling Calibration Effectiveness for CNNs under Varying Noise Levels in Brain Tumour Detection

Ankur Chanda<sup>1</sup>, Kushan Choudhury<sup>1</sup>, Shubhrodeep Roy<sup>1</sup>, Shubhajit Biswas<sup>1</sup> and Dr. Somenath Kuiry<sup>1\*</sup>

<sup>1</sup>Department of CSE(AIML), Institute of Engineering & Management, Kolkata, India

**Abstract.** Accurate confidence estimation in deep learning is essential for high-stakes applications like medical imaging, where overconfident misclassifications can lead to serious consequences. This study looks at how Temperature Scaling (TS), a method used after training, can improve the reliability of CNNs in brain tumor classification. We create a custom CNN and train it on a dataset of brain MRIs. To simulate real-world uncertainty, we add five types of image noise to the test set: Gaussian, Poisson, Salt & Pepper, Speckle, and Uniform. We evaluate model performance using precision, recall, F1-score, accuracy, negative log-likelihood (NLL), and expected calibration error (ECE) both before and after calibration. The results show that TS significantly lowers ECE and NLL under all noise conditions without losing classification accuracy. These findings support the use of TS as an effective and simple approach to improving the decision confidence of medical AI systems, making their outputs more trustworthy in noisy or uncertain environments.

**Keywords:** Temperature Scaling, Confidence Calibration, Brain Tumor Detection, Convolutional Neural Networks (CNNs), Medical Image Classification, Expected Calibration Error (ECE), Negative Log-Likelihood (NLL)

## 1 Introduction

Cancer detection is an important healthcare sector nowadays, and deep learning technologies are among the key elements that help in precision and effectiveness in the detection of diseases. Cancer is a mysterious and fear-inducing disease, or a collection of diseases, in fact, which have been plaguing multicellular life forms for more than 200 million years. A correct and reliable prediction is required in the medical image analysis field; overconfident or misguided decisions might lead to serious clinical consequences. DL techniques, most notably CNNs, have achieved tremendous performance in brain tumor detection from MRI images [2]. Unfortunately, despite being accurate, such models tend to

---

\* Corresponding author: [somenath.kuiry@iem.edu.in](mailto:somenath.kuiry@iem.edu.in)

be badly calibrated and issue probability estimates that are not true likelihoods [10]. This miscalibration erodes trust in high-stakes environments like healthcare and can result in an unwarranted or missed intervention [3].

TS has become a popular post-hoc calibration method due to its simplicity, closed-form optimality, and low computational cost [5,10]. Scaling of confidence in predictions using one temperature parameter in TS brings the predicted probabilities closer to the observed outcomes without degrading the classification accuracy. Although successful in idealized environments, its performance under real imaging conditions has yet to be fully explored. MRI data tend to be contaminated with acquisition hardware noise, motion artifacts from patients, and ambient interference, and thus it is essential to test whether calibration methods continue to be effective in noisy conditions [2,4]. This paper examines the efficacy of TS in calibrating CNNs for classifying brain tumors under various noise scenarios. A light CNN is learned on a composite MRI data set [11] and tested prior to and post using TS on five forms of synthetic noise: Gaussian, Poisson, Salt & Pepper, Speckle, and Uniform. Performance is measured using accuracy, precision, recall, F1-score, Negative Log-Likelihood (NLL), and Expected Calibration Error (ECE). Results demonstrate that TS consistently reduces NLL and ECE across noise scenarios while preserving classification accuracy.

The remainder of this paper is organized as follows: Section II discusses related works on calibration methods and their evolution beyond traditional Temperature Scaling. Section III presents the proposed CNN architecture, dataset details, temperature scaling methodology, and the noise injection strategy. Section IV gives the detailed results of experiments and performance comparisons for varying noise conditions. Finally, the insights of the findings and the directions of future research are presented in Section V.

## 2 Related Works

Calibration of deep neural networks has received growing attention, especially in safety-critical domains such as medical imaging [2,3]. While CNNs can achieve high classification accuracy, they are usually poorly calibrated, with overconfident predictions that erode trustworthiness in practical use [10]. The post-hoc calibration technique aims to make the predicted confidence reflect true correctness.

The most common calibration method due to its simplicity, closed-form optimization, and low computational expense is Temperature Scaling (TS) [5,10]. However, TS is weak in distribution shifts or composition tasks like semantic segmentation. In response to those setbacks, several variants have been proposed. Local Temperature Scaling (LTS) adds pixel-level calibration to TS for spatially aware tasks [6], while Attended Temperature Scaling (ATS) enhances robustness on small or noisy validation sets by putting more emphasis on the strong samples [8]. Adaptive Temperature Scaling (ATS/Adaptive TS) and entropy-based methods further extend calibration by including sample-level adaptations and uncertainty estimations [7,9].

While these advances have been made, most previous research measures calibration against fairly clean data sets, typically avoiding the noisy and artifact-ridden settings present in typical clinical medical imaging [2,4]. This raises the question of whether light calibration techniques like TS remain accurate when MRI scans are corrupted. The present study fills

this void directly by examining TS systematically across five levels of noise to test its resilience for brain tumor identification.

### 3 Proposed Method

#### 3.1 CNN Architecture

In order to conduct binary classification of brain tumor images, we constructed a lightweight Convolutional Neural Network (CNN) optimized for performance and efficiency. The network structure includes four convolutional layers, which are each accompanied by ReLU activation and max-pooling operations to gradually extract spatial hierarchies as well as decrease dimensionality. Two fully connected layers are incorporated after the convolutional blocks for projecting learned features into the classification space. Dropout regularization is applied between the dense layers to avoid overfitting. The output layer generates raw logits, which are transformed into calibrated probability scores after training through temperature scaling. The architecture is optimized in a way that strikes a good balance between computational expense and classification accuracy; thus, it is well-suited for resource-constrained applications, such as edge devices in health care. We have used general data augmentation such as adding noise, random intensity and color modification, and linear corrections.

The model was trained with a batch size of 64 for 60 epochs using a learning rate of 0.0003. For preventing overfitting, a dropout of 0.25 was used between the fully connected layers. The dataset was split, with 80% for training and the remaining 20% was used for testing generalization performance. Training was executed on the PyTorch deep learning system using a high-performance NVIDIA RTX 3050 GPU, supported by 16 GB of system memory.

#### 3.2 Dataset

This model was trained on a composite dataset made from three public repositories: Figshare, SARTAJ brain tumor dataset, and Br35H (Brain Tumor Detection 2020) from Kaggle [11]. Cumulatively, these datasets provide T1-weighted brain MRI images categorized as either tumor or normal. All images were brought to 256 x 256 x 3 resolution, and then pre-processing operations like intensity normalization and margin removal were done. Stratified sampling was employed for the random division of data into training, validation, and test sets to maintain class balance in subsets.

#### 3.3 Temperature Scaling Calibration

Temperature scaling is a post hoc calibration method that can effectively adjust the confidence of the output from a given classifier while preserving accuracy. In this approach, the logits (pre-softmax outputs) of the trained CNN are divided by a scalar temperature parameter,  $T$ , which is trained by minimizing NLL on an independent validation set. The softmax probabilities are computed as:

$$P(\hat{y}) = \frac{e^{z_j/f(T)}}{\sum_j e^{z_j/f(T)}} \quad (1)$$

where ( $z$ ) is the logit vector and ( $T$ ) is the temperature parameter optimized using gradient-based methods. Larger values of ( $T$ ) leads to softer probabilities, but this can help make model confidence align better with true likelihoods. TS was applied to the CNN's output on both clean and noisy test sets to gauge its robustness.

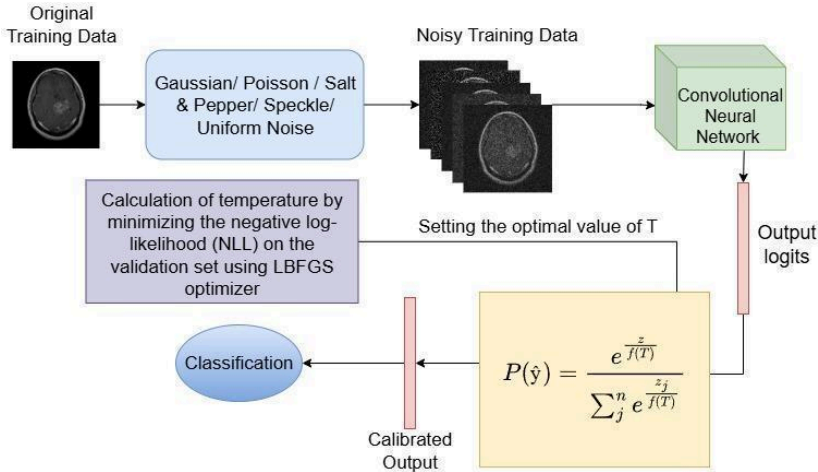


**Fig. 1.** Process Flowchart

Fig. 1 illustrates the flow of the proposed approach, starting with MRI preprocessing and CNN-based feature extraction, followed by the injection of synthetic noise on the test data for simulating real-world scenarios. Afterward, temperature scaling was performed to calibrate prediction confidence. The pipeline concludes with performance evaluation across multiple metrics before and after calibration.

### 3.4 Noise Injection Strategy

To simulate real-world uncertainties in medical imaging, we introduced five types of synthetic noise to the test dataset:

#### 3.4.1 Gaussian Noise

Statistical noise known as normal noise has a probability density function matching that of the normal distribution, sometimes referred to as the Gaussian distribution. Its mean ( $\mu$ ) and variance ( $\sigma^2$ ) define it. The Gaussian noise model is frequently employed in practice and even in circumstances where they are marginally relevant at best because of its mathematical simplicity.

$$P(x) = \frac{1}{\sigma\sqrt{2\pi}} e^{-\frac{(x-\mu)^2}{2\sigma^2}} \quad (2)$$

#### 3.4.2 Impulse Noise

If  $b > a$ , intensity  $b$  will appear as a light dot in the image. Conversely, level  $a$  will appear like a black dot in the image. Therefore, the presence of white and black dots in the picture mimics salt-and-pepper particles, thus also known as **salt-and-pepper noise**.

Unipolar noise is when either  $P_a$  or  $P_b$  is zero. Quick transients like improper switching in cameras or other similar situations cause impulse noise.

$$p(z) = \begin{cases} P_a & \text{for } z = a \\ P_b & \text{for } z = b \\ 0 & \text{otherwise} \end{cases} \quad (3)$$

### 3.4.3 Poisson Noise

Also called photon noise, Poisson noise is a kind of noise resulting from the image sensor's discrete character of photons and electrons. Its prevalent in low-light situations and depends on the signal intensity.

$$P(x) = \frac{\lambda^x e^{-\lambda}}{x!} \quad (4)$$

where  $P(x)$  is the likelihood of seeing  $x$  photons or electrons, and  $\lambda$  is the mean number of photons or electrons (mean of the distribution).

### 3.4.4 Speckle Noise

Usually affecting coherent imaging systems like radar, ultrasound, and laser, speckle noise is a multiplicative noise. The interference of coherent waves reflected from several surfaces causes this noise, which gives the picture a grainy look.

A natural characteristic of medical ultrasound imaging, speckle noise usually lowers the image quality and contrast, hence lowering the diagnostic utility of this imaging tool.

$$I_{noisy}(x, y) = I_{clean}(x, y) \cdot N(x, y) \quad (5)$$

where  $I_{noisy}(x, y)$  is the noisy picture,  $I_{clean}(x, y)$  is the original clean image, and  $N(x, y)$  is a noise term that follows a multiplicative model, often modeled as a Rayleigh or Gamma distribution.

### 3.4.5 Uniform Noise

Uniform noise is noise that follows a uniform distribution, hence every value within a given range is equally probable.

$$P(x) = \frac{1}{b-a}, a \leq x \leq b \quad (6)$$

where  $P(x)$  is the likelihood of seeing  $x$  photons or electrons, and  $\lambda$  is the mean number of photons or electrons (mean of the distribution).

where  $P(x)$  is the probability density function.

Respectively,  $a$  and  $b$  are the lowest and maximum range values.

## 4 Results and Discussion

### 4.1 Experimental Setup

Python was used to implement all models; Pytorch was the main deep learning framework. Training was done on a machine with 16 GB RAM and an NVIDIA RTX 3050 GPU. Using the Adam optimizer with a learning rate of  $3e^{-4}$ , a batch size of 64, and a maximum of 60

epochs, the CNN model was trained. Overfitting was avoided by early stopping. To improve generalization, dropout layers were applied at a 0.25 rate.

Using the L-BFGS optimization technique, the best temperature parameter ( $T$ ) was found by reducing the Negative Log-Likelihood (NLL) loss. The unmodified test set and noise-corrupted test sets were used to assess all calibration studies.

## 4.2 Evaluation Metrics

The following criteria were used to evaluate the model's performance:

- Accuracy: Total percentage of accurate forecasts

$$Accuracy = \frac{TP+TN}{TP+TN+FP+FN} \quad (7)$$

- Precision: Ratio of actual positive forecasts among all positive forecasts

$$Precision = \frac{TP}{TP+FP} \quad (8)$$

- Recall: Percentage of true positive forecasts among all actual positives.

$$Recall = \frac{TP}{TP+FN} \quad (9)$$

- F1-Score: Harmonic mean of precision and recall.

$$F1 - Score: \frac{2 \cdot (Precision \cdot Recall)}{(Precision + Recall)} \quad (10)$$

- Negative Log-Likelihood (NLL): Assesses how closely the projected probability distribution matches actual labels.

$$NLL = - \sum_{i=1}^n \log(\hat{\pi}(y_i|x_i)) \quad (11)$$

- Expected Calibration Error (ECE): Measures the difference between projected confidence and actual accuracy across bins.

$$ECE = \sum_{m=1}^M \frac{|B_m|}{n} |acc(B_m) - conf(B_m)| \quad (12)$$

## 4.3 Results without Noise (Baseline)

**Table 1.** Baseline model performance before and after calibration

Strategy	Precision	Recall	f1-score	Accuracy	NLL	ECE
Before Calibration	0.98	0.975	0.98	0.98	0.079	0.016
After Calibration	0.9875	0.975	0.975	0.98	0.077	0.017

The model demonstrated strong performance prior to the introduction of noise. Remarkably, the number of false positives was 8 both prior to and after calibration. However, as seen in Fig. 2, the number of false negatives increased somewhat, from 11 to 13.

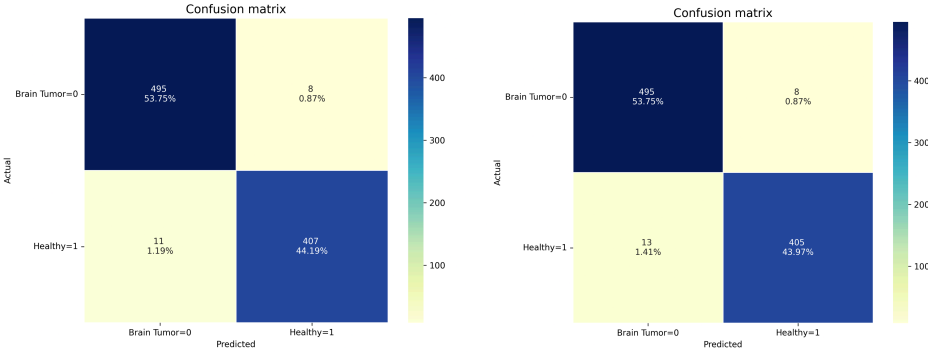


**Fig. 2.** Confusion matrix of the baseline model before & after temperature

Application of temperature scaling does not improve performance metrics like accuracy, F1-score, recall, and precision; rather, it leads to a minor reduction in these values, as shown in Table I. The small dataset size can be the cause of this effect since it might limit the efficiency of post-hoc calibration techniques, such as temperature scaling. Moreover, the complex model structure might already effectively capture the underlying data distribution in a way that additional calibration would be redundant or even detrimental in this particular case.

**4.4 Calibration Performance under Various Noise Conditions**

**Table 2.** Comparing calibration performance under Gaussian noise.

Metric	Gaussian Noise						
	$\mu=0.0, \sigma=0.02$	$\mu=0.0, \sigma=0.05$	$\mu=0.0, \sigma=0.1$	$\mu=0.0, \sigma=0.2$	$\mu=0.1, \sigma=0.2$	$\mu=0.1, \sigma=0.3$	$\mu=0.2, \sigma=0.3$
Uncalibrated							
Prec	0.98	0.985	0.97	0.975	0.965	0.96	0.965
Rec	0.98	0.98	0.965	0.97	0.965	0.955	0.95
F1	0.98	0.985	0.965	0.975	0.965	0.955	0.965
TP	490	497	496	494	488	485	477
FN	13	6	7	9	15	18	26
FP	3	9	23	15	17	20	16
TN	415	409	395	403	401	398	402
NLL	0.065	0.075	0.127	0.085	0.093	0.069	0.108
ECE	0.010	0.012	0.021	0.019	0.013	0.017	0.020
Calibrated							
Prec	0.985	0.985	0.955	0.975	0.975	0.975	0.98
Rec	0.98	0.99	0.955	0.975	0.97	0.975	0.955
F1	0.98	0.985	0.955	0.975	0.975	0.975	0.965
TP	494	496	488	497	490	490	479
FN	9	7	15	6	13	13	24
FP	7	6	23	18	12	12	10
TN	411	412	395	400	406	406	408
NLL	0.060	0.061	0.113	0.076	0.089	0.067	0.093
ECE	0.007	0.006	0.009	0.013	0.011	0.014	0.013
Optimal Temperature							

Metric	Gaussian Noise						
	$\mu=0.0,$ $\sigma=0.02$	$\mu=0.0,$ $\sigma=0.05$	$\mu=0.0,$ $\sigma=0.1$	$\mu=0.0,$ $\sigma=0.2$	$\mu=0.1,$ $\sigma=0.2$	$\mu=0.1,$ $\sigma=0.3$	$\mu=0.2,$ $\sigma=0.3$
Uncalibrated							
Prec	0.98	0.985	0.97	0.975	0.965	0.96	0.965
Rec	0.98	0.98	0.965	0.97	0.965	0.955	0.95
F1	0.98	0.985	0.965	0.975	0.965	0.955	0.965
TP	490	497	496	494	488	485	477
FN	13	6	7	9	15	18	26
FP	3	9	23	15	17	20	16
TN	415	409	395	403	401	398	402
NLL	0.065	0.075	0.127	0.085	0.093	0.069	0.108
ECE	0.010	0.012	0.021	0.019	0.013	0.017	0.020
Calibrated							
Prec	0.985	0.985	0.955	0.975	0.975	0.975	0.98
Rec	0.98	0.99	0.955	0.975	0.97	0.975	0.955
Optimal Temp	1.499	1.581	1.532	1.501	1.499	1.261	1.540

#### 4.4.1 Gaussian Noise

The comparison between various Gaussian noise conditions (Table 2) highlights that calibration significantly improves the NLL and ECE scores without affecting the prediction performance metrics such as precision, recall, and F1-score. These metrics remain high in all noisy conditions; however, the best calibrated scores occur at  $\mu = 0.0, \sigma = 0.02$ , where the best precision-recall trade-off and optimal calibration performance are found with an optimal temperature of 1.499. Optimal temperature ranges from 1.261 to 1.581 depending on the extent of Gaussian noise. The smallest optimal temperature of 1.261 corresponds to  $\mu = 0.1, \sigma = 0.3$ , suggesting the necessity of more conservative smoothing under more extreme noise conditions. Conversely, the highest optimal temperature of 1.581 corresponds to  $\mu = 0.0, \sigma = 0.05$ , suggesting that greater softening of prediction confidence was required in this configuration.

#### 4.4.2 Poisson Noise and Salt & Pepper Noise

**Table 3.** Comparing calibration performance under Poisson and Salt & Pepper noise.

Metric	Poisson			Salt & Pepper		
	scale = 0.5	scale = 1	scale = 2	salt_prob = 0.02 pepper_prob = 0.02	salt_prob = 0.1 pepper_prob = 0.1	salt_prob = 0.2 pepper_prob = 0.2
Uncalibrated						
Prec	0.97	0.975	0.975	0.965	0.945	0.97
Rec	0.965	0.975	0.98	0.96	0.945	0.965
F1	0.97	0.975	0.975	0.965	0.945	0.965
TP	485	495	491	485	478	493
FN	18	8	12	18	25	10

FP	11	13	10	16	23	19
TN	407	405	408	402	395	399
NLL	0.096	0.067	0.082	0.139	0.149	0.138
ECE	0.010	0.010	0.011	0.02	0.009	0.018
Calibrated						
Prec	0.985	0.98	0.98	0.955	0.95	0.975
Rec	0.97	0.98	0.98	0.96	0.95	0.97
F1	0.975	0.98	0.98	0.955	0.95	0.975
TP	486	496	493	482	477	490
FN	17	7	10	21	26	13
FP	8	10	10	18	20	12
TN	410	408	408	400	398	406
NLL	0.091	0.065	0.076	0.131	0.145	0.129
ECE	0.012	0.010	0.011	0.013	0.017	0.017
Optimal Temperature						
Optimal Temp	1.435	1.382	1.452	1.469	1.399	1.499

For Poisson noise, the configuration with scale = 1 is found to be optimal in terms of balancing prediction quality and calibration, achieving an optimal temperature of 1.382 (refer to Table 3). In the case of Salt & Pepper noise, calibration performance is well-maintained even as noise levels increase. The configuration with salt\_prob = 0.2 and pepper\_prob = 0.2 yields the highest F1-score and the lowest NLL (0.126) among its group, at an optimal temperature of 1.499.

#### 4.4.3 Uniform and Speckle noise

**Table 4.** Comparing calibration performance under Speckle & Uniform noise.

Metric	Speckle scale = 0.01	Speckle scale = 0.05	Speckle scale = 0.1	Uniform scale = 0.02	Uniform scale = 0.05	Uniform scale = 0.1
Uncalibrated						
Prec	0.98	0.97	0.98	0.98	0.975	0.98
Rec	0.985	0.97	0.98	0.98	0.975	0.98
F1	0.98	0.97	0.98	0.98	0.975	0.98
TP	491	493	493	495	495	491
FN	12	10	10	8	8	12
FP	5	18	9	8	13	7
TN	413	400	409	410	405	411
NLL	0.067	0.058	0.082	0.062	0.058	0.081
ECE	0.007	0.007	0.012	0.001	0.009	0.008
Calibrated						
Prec	0.98	0.975	0.98	0.985	0.985	0.98
Rec	0.98	0.975	0.98	0.98	0.98	0.985
F1	0.98	0.975	0.98	0.985	0.985	0.98
TP	491	494	493	495	495	491

FN	12	9	10	8	8	12
FP	7	13	9	7	7	6
TN	411	405	409	411	411	412
NLL	0.064	0.06	0.07	0.054	0.055	0.082
ECE	0.006	0.009	0.006	0.007	0.007	0.015
Optimal Temperature						
Optimal Temp	1.399	1.175	1.564	1.501	1.425	1.314

The results for Uniform and Speckle noise are shown in Table 4. From the table we can see that, Temperature scaling consistently reduces NLL and ECE, even with increasing noise levels; maintains or slightly improves F1-scores, and suggests that lower optimal temperatures are sufficient under light noise levels (scale = 0.01-0.05), whereas higher temperatures (above 1.5) are necessary under heavier noise conditions.

#### 4.5 Further Analysis

We extended our experiments to a more robust architecture, ResNet50, using the most optimal noise parameters identified from earlier experiments to test the effectiveness of TS on deeper models. The results are summarised in Table 5 below.

**Table 5.** Comparing calibration performance of ResNet50 under optimal noise parameters

Metric	Gaussian ( $\mu=0.0$ , $\sigma=0.02$ )	Poisson (scale=1)	Salt & Pepper (salt=0.2, p=0.2)	Speckle (scale=0.05)	Uniform (scale=0.05)
Uncalibrated					
Prec	0.995	0.995	0.99	0.99	0.99
Rec	0.99	0.995	0.99	0.99	0.99
F1	0.99	0.99	0.99	0.99	0.99
TP	497	501	499	495	500
FN	6	2	4	8	3
FP	3	2	5	4	5
TN	415	417	413	414	413
NLL	0.027	0.015	0.026	0.024	0.017
ECE	0.008	0.004	0.007	0.006	0.007
Calibrated					
Prec	0.995	0.995	0.99	0.99	1.00
Rec	0.995	0.995	0.99	0.99	1.00
F1	0.99	0.995	0.99	0.99	1.00
TP	500	503	500	495	503
FN	3	0	3	8	0
FP	1	2	3	5	0
TN	417	417	415	415	418
NLL	0.025	0.014	0.024	0.025	0.015
ECE	0.003	0.003	0.003	0.006	0.006
Optimal Temperature					

Metric	Gaussian ( $\mu=0.0$ , $\sigma=0.02$ )	Poisson (scale=1)	Salt & Pepper (salt=0.2, p=0.2)	Speckle (scale=0.05)	Uniform (scale=0.05)
Uncalibrated					
Prec	0.995	0.995	0.99	0.99	0.99
Rec	0.99	0.995	0.99	0.99	0.99
F1	0.99	0.99	0.99	0.99	0.99
TP	497	501	499	495	500
FN	6	2	4	8	3
FP	3	2	5	4	5
TN	415	417	413	414	413
NLL	0.027	0.015	0.026	0.024	0.017
ECE	0.008	0.004	0.007	0.006	0.007
Calibrated					
Prec	0.995	0.995	0.99	0.99	1.00
Rec	0.995	0.995	0.99	0.99	1.00
Optimal Temp	1.321	1.290	1.321	1.316	1.218

In comparing performance, we observe that temperature scaling really improves both the false positive (FP) and false negative (FN) rates for ResNet, while leaving overall model accuracy unaffected and also reducing the NLL loss and ECE. These findings suggest that the benefits of calibration methods such as temperature scaling are not confined to simple CNN baselines, but can also enhance the performance of deeper, state-of-the-art architectures.

## 5 Conclusion

Temperature Scaling (TS) is a simple, efficient post-training calibration method enhancing model reliability against different noises, including Gaussian, Poisson, Salt & Pepper, Speckle, and Uniform noise. Experimental results demonstrate significant reduction in model miscalibration using TS, exhibiting large improvements over several of the major calibration metrics such as NLL and ECE. Interestingly, this is achieved without degrading the quality of predictions since other important performance metrics such as precision, recall, F1-score, and overall accuracy are robust for all noise settings. These results, therefore, show that TS can be an effective but light model confidence booster facility, which is relevant for sensitive tasks like medical diagnosis, where the decision needs to be accurate and trustworthy. In our future studies, we would like to study how different calibration methods, such as TS and others, perform on a wide range of modern deep learning models on much larger datasets for generalization. Specifically, we want to see how well they perform in terms of reducing both false negatives and false positives and, crucially, why both are so particularly valuable in high-risk domains such as medicine. We will also extend the research by comparing Temperature Scaling with other state-of-the-art calibration techniques, namely Adaptive Temperature Scaling, Entropy-Based Temperature Scaling, and Sample-Dependent methods. The application of such techniques will enable a more thorough assessment of the effectiveness of various calibration techniques, particularly in the presence of fluctuating noise and distributional drift in medical image

data. This path will allow for the advancement of our understanding of how calibrated confidence scores can lead to safer and more accurate results as well as increased confidence in forecasts.

## References

1. Siegel, Rebecca L., Angela N. Giaquinto, and Ahmedin Jemal. "Cancer statistics, (2024)." *CA: a cancer journal for clinicians* **74**, no. 1 (2024).
2. Babu Vimala, B., Srinivasan, S., Mathivanan, S. K., Mahalakshmi, Jayagopal, P., & Dalu, G. T. (2023). Detection and classification of brain tumor using hybrid deep learning models. *Scientific reports*, **13**(1), 23029. <https://doi.org/10.1038/s41598-023-50505-6>
3. Pashayan, N., & Pharoah, P. D. P. (2020). The challenge of early detection in cancer. *Science* (New York, N.Y.), **368**(6491), 589–590. <https://doi.org/10.1126/science.aaz2078>.
4. Ma Y, Peng Y, Wu T-Y, Balas VE. Transfer learning model for false positive reduction in lymph node detection via sparse coding and deep learning. *Journal of Intelligent & Fuzzy Systems*. (2022);43(2):2121-2133. doi:10.3233/JIFS-219312
5. Balanya, S.A., Maroñas, J. & Ramos, D. Adaptive temperature scaling for Robust calibration of deep neural networks. *Neural Comput & Applic* **36**, 8073–8095 (2024). <https://doi.org/10.1007/s00521-024-09505-4>
6. Ding, Zhipeng & Han, Xu & Liu, Peirong & Niethammer, Marc. (2020). Local Temperature Scaling for Probability Calibration. 10.48550/arXiv.2008.05105.
7. Joy, Tom & Pinto, Francesco & Lim, Ser-Nam & Torr, Philip & Dokania, Puneet. (2023). Sample-Dependent Adaptive Temperature Scaling for Improved Calibration. *Proceedings of the AAAI Conference on Artificial Intelligence*. 37. 14919-14926. 10.1609/aaai.v37i12.26742.
8. Mozafari, Azadeh & Gomes, Hugo & Leão Neto, Wilson & Janny, Steeven & Gagné, Christian. (2019). Attended Temperature Scaling: A Practical Approach for Calibrating Deep Neural Networks.
9. Balanya, Sergio & Maroñas, Juan & Ramos, Daniel. (2024). Adaptive temperature scaling for Robust calibration of deep neural networks. *Neural Computing and Applications*. 36. 1-23. 10.1007/s00521-024-09505-4.
10. Guo, Chuan & Pleiss, Geoff & Sun, Yu & Weinberger, Kilian. (2017). On Calibration of Modern Neural Networks. 10.48550/arXiv.1706.04599.
11. Sartaj Bhuvaji, Ankita Kadam, Prajakta Bhumkar, Sameer Dedge, and Swati Kanchan. (2020). Brain Tumor Classification (MRI) [Data set]. *Kaggle*. <https://doi.org/10.34740/KAGGLE/DSV/1183165>